

Going beyond the Kaiser redshift-space distortion formula: a full general relativistic account of the effects and their detectability in galaxy clustering

Jaiyul Yoo^{1,2,*}, Nico Hamaus¹, Uroš Seljak^{1,2,3,4}, and Matias Zaldarriaga⁵

¹*Institute for Theoretical Physics, University of Zürich, CH-8057 Zürich, Switzerland*

²*Lawrence Berkeley National Laboratory, University of California, Berkeley, CA 94720, USA*

³*Physics Department and Astronomy Department, University of California, Berkeley, CA 94720, USA*

⁴*Institute for the Early Universe, Ewha Womans University, 120-750 Seoul, South Korea and*

⁵*School of Natural Sciences, Institute for Advanced Study, Einstein Drive, Princeton, NJ 08540, USA*

Kaiser redshift-space distortion formula describes well the clustering of galaxies in redshift surveys on small scales, but there are numerous additional terms that arise on large scales. Some of these terms can be described using Newtonian dynamics and have been discussed in the literature, while the others require proper general relativistic description that was only recently developed. Accounting for these terms in galaxy clustering is the first step toward tests of general relativity on horizon scales. The effects can be classified as two terms that represent the velocity and the gravitational potential contributions. Their amplitude is determined by effects such as the volume and luminosity distance fluctuation effects and the time evolution of galaxy number density and Hubble parameter. We compare the Newtonian approximation often used in the redshift-space distortion literature to the fully general relativistic equation, and show that Newtonian approximation accounts for most of the terms contributing to velocity effect. We perform a Fisher matrix analysis of detectability of these terms and show that in a single tracer survey they are completely undetectable. To detect these terms one must resort to the recently developed methods to reduce sampling variance and shot noise. We show that in an all-sky galaxy redshift survey at low redshift the velocity term can be measured at a few sigma if one can utilize halos of mass $M \geq 10^{12} h^{-1} M_{\odot}$ (this can increase to $10\text{-}\sigma$ or more in some more optimistic scenarios), while the gravitational potential term itself can only be marginally detected. We also demonstrate that the general relativistic effect is not degenerate with the primordial non-Gaussian signature in galaxy bias, and the ability to detect primordial non-Gaussianity is little compromised.

PACS numbers: 98.80.-k, 98.65.-r, 98.80.Jk, 98.62.Py

I. INTRODUCTION

In the past few decades galaxy redshift surveys have been one of the indispensable tools in cosmology, covering a progressively larger fraction of the sky with increasing redshift depth. With the upcoming dark energy surveys this trend will continue in the future. However, despite the advance in observational frontiers, there remained a few unanswered questions in the theoretical description of galaxy clustering. One is the issue of validity of the Kaiser formula, where density perturbation in redshift space is density perturbation in real space multiplied with a term that depends on the angle between the line-of-sight direction and the direction of the Fourier mode (we give a more detailed definition below) [1]. It has been well known (e.g., [2]) that the simplest version omits some of the terms coming from the Jacobian of the transformation from real space to redshift space, terms of order $v/\mathcal{H}r$, where v is the velocity and r is the distance to the galaxy and \mathcal{H} is the conformal Hubble parameter. It is argued that these terms are potentially important, especially for large angular separations (e.g., see, [3–7]), but most of the analyses so far have focused on effects in correlation function, without proper signal-to-noise analysis (see, however, [8]).

A second, related issue, is whether the terms originally derived in the Newtonian approximation, get modified when

a proper general relativistic description is employed. On horizon scales, the standard Newtonian description naturally breaks down, and a choice of hypersurface of simultaneity becomes an inevitable issue, demanding a fully relativistic treatment of galaxy clustering beyond the current Newtonian description. In recent work [9, 10], it is shown that a proper relativistic description can be easily obtained by following the observational procedure in constructing the galaxy fluctuation field and its statistics: We need to model observable quantities, rather than theoretically convenient but unobservable quantities, usually adopted in the standard method. While both the relativistic and the standard Newtonian descriptions are virtually indistinguishable in the Newtonian limit, they are substantially different on horizon scales, rendering galaxy clustering measurements a potential probe of general relativity.

The relativistic description of galaxy clustering includes two new terms that scale as velocity and gravitational potential. Compared to the dominant density contribution, they are suppressed by \mathcal{H}/k and $(\mathcal{H}/k)^2$ and become important only on large scales, where the comoving wavevector amplitude is k . Consequently, the identification of these terms just by looking at the galaxy power spectrum is hampered because of sampling variance, and the general relativistic effects unaccounted in the standard Newtonian description may result in systematic errors less than $1\text{-}\sigma$ for most of the volume available at $z \lesssim 3$ in the standard power spectrum analysis [10]. We revisit this calculation here, using a more realistic description of these terms, but the basic conclusion remains the same.

*jyoo@physik.uzh.ch

In light of the fact that these corrections to the Kaiser formula provide a potential probe of the consistency of our model, including generic tests of general relativity on large scales, it is worth exploring if these terms can be observed. A new multi-tracer method [11] takes advantage of the fact that differently biased galaxies trace the same underlying matter distribution, and it can be used to cancel the randomness of the matter distribution in a single realization of the Universe, eliminating the sampling variance limitation. This method has been used in [12] to investigate the velocity effects of [9, 10], noting that for any given Fourier mode the imaginary part of velocity couples to the real part of density and vice versa. Even with this novel technique, the expected detection level is low [12].

If sampling variance is eliminated, the dominant remaining source of error is shot noise, caused by the discrete nature of galaxies. Recently, a shot noise cancelling technique has been proposed [13] and investigated for detecting primordial non-Gaussianity [14] in combination with the sampling variance cancelling technique. The basis of the method is that by using halo mass dependent weights one can approximate a halo field as the dark matter field and reduce the stochasticity between them. While this works best when comparing halos to dark matter, some shot noise cancelling can also be achieved by comparing halos to each other [14, 15]. This opens up a new opportunity to probe horizon scales and extract cosmological information with higher signal-to-noise ratio.

In this work our primary goal is to explore the detectability of these effects in galaxy clustering on cosmological horizon scales using the galaxy power spectrum measurements with both single tracer technique and with the multi-tracer and shot noise cancelling techniques. In addition we clarify the relation of the galaxy fluctuation field often used in the redshift-space distortion literature using Newtonian approximation to the fully general relativistic equation. Finally, we also investigate the impact of the general relativistic effects in detecting the primordial non-Gaussian signature in galaxy bias.

The organization of the paper is as follows. In Sec. II, we present the full general relativistic description of galaxy clustering. In Sec. III, we discuss the Newtonian correspondence and its relation to the redshift-space distortion literature. The multi-tracer and shot noise cancelling techniques are presented in Sec. IV. In Sec. V, we provide the measurement significance of the general relativistic effects in the galaxy power spectrum. In Sec. VI, we extend our formalism to the primordial non-Gaussianity. Finally, we discuss the implication of our results in Sec. VII.

II. GENERAL RELATIVISTIC DESCRIPTION OF GALAXY CLUSTERING

A full general relativistic description of galaxy clustering is developed in [9, 10] (see also [16–18]). Previously, we have adopted the simplest linear bias ansatz, in which the galaxy number density is just a function of the matter den-

sity $n_g = F[\rho_m]$, both at the same spacetime.¹ However, this ansatz turns out to be rather restrictive, since the time evolution of the galaxy sample is entirely driven by the evolution of the matter density $\propto (1+z)^3$. Here we make one modification in the adopted linear bias ansatz by relaxing this assumption and providing more freedom, while keeping the locality. We allow the galaxy number density at the same matter density to differ depending on its local history, as a local observer at the galaxy formation site is affected by its local matter density and the proper time to the linear order in perturbation, i.e., $n_g = F[\rho_m, t_p]$ with t_p being the proper time measured in the galaxy rest frame. Physically, the presence of long wavelength modes affects the local dynamics of galaxy formation by changing the local curvature and thus the expansion rate, and these are modulated by the Laplacian of the comoving curvature and the proper time [19]. Therefore, in addition to the contribution of the matter density fluctuation $m_{\delta z} = \delta - 3\delta z$ at the observed redshift z [9, 10], the physical number density of galaxies has additional contribution from the distortion between the observed redshift and the proper time, when expressed at the observed redshift:

$$\begin{aligned} n_g &= \bar{n}_g(z) [1 + b(\delta - 3\delta z) - b_t \delta z_v] \\ &= \bar{n}_g(z) [1 + b\delta_v - e\delta z_v], \end{aligned} \quad (1)$$

where the matter density fluctuation is δ , the lapse δz in the observed redshift z is defined as $1+z = (1+\bar{z})(1+\delta z)$, and the homogeneous redshift parameter is related to the cosmic expansion factor as $1/a = 1 + \bar{z}$. The subscript v indicates quantities are evaluated in the dark matter comoving gauge.²

The galaxy bias factor is $b = \partial \ln \bar{n}_g / \partial \ln \rho_m|_{t_p}$ and the time evolution of the galaxy number density due to its local history is $b_t = \partial \ln \bar{n}_g / \partial \ln(1+z)|_{\rho_m}$. Therefore, the total time evolution of the mean galaxy number density is proportional to the evolution bias [21],

$$e = \frac{d \ln \bar{n}_g}{d \ln(1+z)} = 3b + b_t. \quad (2)$$

For galaxy samples with constant comoving number density, the evolution bias factor is $e = 3$ due to our use of the physical number density in Eq. (2). This biasing scheme in Eq. (1) is consistent with [16–19, 22], and our previous bias ansatz corresponds to $b_t = 0$.

¹ On large scales, a more general stochastic relation between the galaxy number density and the matter density also reduces to the local form we adopted here [11]. As opposed to some confusion in literature, this biasing scheme is independent of whether galaxies are observed.

² Gauge-dependence arises, only when perturbation quantities are considered. For example, the physical number density of galaxies is a well-defined scalar field without gauge ambiguity. However, when we split it into the homogeneous part and the perturbation part, the correspondence of the physical quantity to the homogeneous part depends on the coordinate choice, and consequently the perturbation part becomes gauge-dependent [20]. The comoving gauge is a choice of gauge conditions, in which $v = 0$ or the off-diagonal component of the energy-momentum tensor is zero. No simple choice of gauge conditions corresponds to the observer's choice of coordinates (z, θ, ϕ) .

Therefore, with this more physically motivated bias ansatz, the general relativistic description of the observed galaxy fluctuation is [9, 10]

$$\begin{aligned} \delta_{\text{obs}} &= [b \delta_v - e \delta z_v] + \alpha_\chi + 2 \varphi_\chi + V + 3 \delta z_\chi \\ &+ 2 \frac{\delta r_\chi}{r} - H \frac{d}{dz} \left(\frac{\delta z_\chi}{\mathcal{H}} \right) - 5p \delta \mathcal{D}_L - 2 \mathcal{K}. \end{aligned} \quad (3)$$

Here the luminosity function slope of the source galaxy population at the threshold is p . Note that this is the slope of the luminosity function, expressed in terms of absolute magnitude $M = \text{constant} - 2.5 \log L$, hence the factor $5p$ instead of the factor $2\alpha_L$, where α_L is the slope of the luminosity function expressed in terms of luminosity L [see Eq. (23)]. In addition, the comoving line-of-sight distance to the observed redshift is r , the dimensionless fluctuation in the luminosity distance is $\delta \mathcal{D}_L$, the temporal and spatial metric perturbations are α_χ and φ_χ , the line-of-sight velocity is V , and the gauge-invariant radial displacement and lensing convergence are δr_χ and \mathcal{K} .³ The subscript χ indicates quantities are evaluated in the conformal Newtonian gauge (also known as the zero-shear $\chi = 0$ gauge).⁴ We have ignored the vector and tensor contributions to δ_{obs} in Eq. (3).

We emphasize that compared to [9, 10] it is only the terms in the square bracket that are affected by the choice of linear bias ansatz, and Eq. (3) is consistent with [16–19, 22]. Various other terms in Eq. (3) arise due to the mismatch between the observed and the physical quantities. The radial and angular distortions are represented by δr_χ and \mathcal{K} , and the distortion in the observed redshift corresponds to the derivative term. The conversion of physical volume to comoving volume gives rise to the distortion $3 \delta z_\chi$, and the rest of the potential and velocity terms defines the local Lorentz frame, where the source galaxies are defined. For galaxy samples selected by the observed flux, additional contribution $5p \delta \mathcal{D}_L$ arises. Further discussion regarding this contribution is given later in this section.

Since Eq. (3) is written in terms of gauge-invariant variables, it can be evaluated with any choice of gauge conditions. However, in evaluating Eq. (3), it proves convenient to use different combinations of gauge-invariant variables, rather than to choose one specific gauge condition and convert all the gauge-invariant variables in Eq. (3) to quantities in the chosen gauge.

³ The displacement of the source galaxy position from the observed galaxy position is split into the radial and angular components, and these two parts are expressed in terms of gauge-invariant quantities, i.e., their forms differ in each gauge choice but give the same value regardless of gauge choice. These quantities are most conveniently expressed in the conformal Newtonian gauge. In [10] the radial distortion is denoted as $\delta \mathcal{R}$. Here we use a slightly different notation for the radial distortion δr_χ to avoid confusion with the dimensionless coefficient \mathcal{R} in Eq. (21).

⁴ The covariant derivative of the observer velocity is often decomposed into expansion, shear, rotation, and acceleration vectors [23]. The shear component is proportional to $\chi = a(\beta + \gamma')$ with the metric convention in [10]. The conformal Newtonian gauge or the zero-shear gauge corresponds to the frame, in which there is no shear seen by an observer moving orthogonal to the constant-time hypersurface.

For a pressureless medium in a flat universe, the Einstein equations are (e.g., [20, 23, 24])

$$k^2 \varphi_\chi = \frac{3H_0^2}{2} \Omega_m \frac{\delta v}{a}, \quad (4)$$

$$\varphi'_v = \mathcal{H} \alpha_v, \quad (5)$$

$$\alpha_\chi = -\varphi_\chi, \quad (6)$$

and the conservation equations are

$$v'_\chi + \mathcal{H} v_\chi = k \alpha_\chi, \quad (7)$$

$$\delta'_v = -3\varphi'_v - k v_\chi, \quad (8)$$

where the prime is a derivative with respect to the conformal time τ and the equations are in Fourier space. From these equations, it is well-known that the dark-matter comoving gauge ($v = 0$) is coincident with synchronous gauge [$\alpha_\chi = \alpha_v + (av_\chi)' / ak$, hence $\alpha_v = 0$ from Eq. (7)] and the comoving curvature is conserved ($\varphi'_v = 0$) [25, 26]. Furthermore, since these gauge-invariant variables correspond to the usual Newtonian quantities [25, 27], hereafter we adopt a simple notation $\delta v \equiv \delta_m$, $v_\chi \equiv v$, and $\varphi_\chi = -\alpha_\chi \equiv \phi$ to emphasize their connection.

To facilitate evaluation of Eq. (3), we express the remaining gauge-invariant quantities in terms of δ_m , v , and ϕ as

$$V = \frac{\partial}{\partial r} \int \frac{d^3 \mathbf{k}}{(2\pi)^3} \frac{-v(\mathbf{k})}{k} e^{i\mathbf{k} \cdot \mathbf{x}}, \quad (9)$$

$$\delta z_\chi = V + \phi + \int_0^r d\tilde{r} 2\phi', \quad (10)$$

$$\delta z_v = \delta z_\chi + \int \frac{d^3 \mathbf{k}}{(2\pi)^3} \frac{\mathcal{H} v}{k} e^{i\mathbf{k} \cdot \mathbf{x}}, \quad (11)$$

$$\delta r_\chi = -\frac{\delta z_\chi}{\mathcal{H}} - \int_0^r d\tilde{r} 2\phi, \quad (12)$$

$$\mathcal{K} = -\int_0^r d\tilde{r} \left(\frac{r - \tilde{r}}{\tilde{r}} \right) \hat{\nabla}^2 \phi, \quad (13)$$

$$\begin{aligned} \delta \mathcal{D}_L &= \phi + V - \frac{\delta z_\chi}{\mathcal{H} r} + \int_0^r d\tilde{r} \frac{\tilde{r}}{r} 2\phi' - \frac{1}{r} \int_0^r d\tilde{r} 2\phi \\ &+ \int_0^r d\tilde{r} \frac{(r - \tilde{r})}{r} \tilde{r} \left(\Delta \phi + \phi'' - 2 \frac{\partial \phi'}{\partial \tilde{r}} \right) \\ &= \frac{\delta r_\chi}{r} + \delta z_\chi + \varphi_\chi - \mathcal{K}, \end{aligned} \quad (14)$$

$$\begin{aligned} -H \frac{d}{dz} \left(\frac{\delta z_\chi}{\mathcal{H}} \right) &= -V - \frac{1+z}{H} \phi' - \frac{1+z}{H} \frac{\partial V}{\partial r} \\ &- \delta z_\chi + \frac{1+z}{H} \frac{dH}{dz} \delta z_\chi, \end{aligned} \quad (15)$$

where integration by part is performed in Eq. (14) and we have ignored quantities at origin that can be absorbed to the observed mean [9, 10]. The total derivative in Eq. (15) is with respect to the observed redshift z and it is related to the null geodesic as

$$\frac{d}{dz} = \frac{1}{H} \frac{d}{dr} = -\frac{1}{H} \left(\frac{\partial}{\partial \tau} - \frac{\partial}{\partial r} \right). \quad (16)$$

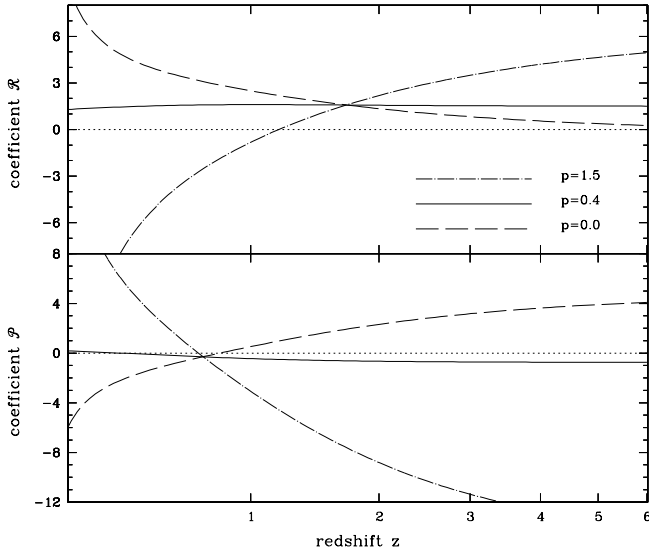


FIG. 1: Redshift dependence of two dimensionless parameters \mathcal{R} and \mathcal{P} in Eq. (21). Non-vanishing values of \mathcal{R} and \mathcal{P} represent the general relativistic effects in galaxy clustering, each of which describes the contributions of the gravitational potential and the velocity to the observed galaxy fluctuation field. Three different curves represent galaxy samples in a volume-limited survey (p is constant) with three different limits L_t in luminosity threshold: a sample with low threshold $L_t \ll L_*$ ($p = 0$; dashed), a sample with no magnification bias $L_t \simeq L_*$ ($p = 0.4$; solid), a sample at high luminosity tail $L_t \gg L_*$ ($p = 1.5$; dot-dashed). The evolution bias factor $e = 3$ is fixed in all cases, representing homogeneous galaxy samples (constant comoving number density) often constructed in large-scale galaxy surveys.

The derivative term also appeared as a partial derivative in [9, 10], while we wrote it here as a total derivative to imply Eq. (16). However, in a sense it is a partial derivative with respect to the observed redshift with other observable quantities (θ, ϕ) kept fixed.

The observed galaxy fluctuation in Eq. (3) is the sum of the matter density δ_m , the gravitational potential ϕ , the line-of-sight velocity V , and other distortions such as δz_χ , δr_χ , and $\delta \mathcal{D}_L$, and they are also a linear combination of δ_m , ϕ , and V with various prefactors and integrals in Eqs. (9)–(15), which in turn can be expressed in terms of the matter density δ_m . Using the Einstein equations, we have

$$\phi = \frac{3H_0^2}{2} \frac{\Omega_m}{ak^2} \delta_m, \quad (17)$$

$$v = -\frac{1}{k} \delta'_m = -\frac{\mathcal{H}f}{k} \delta_m, \quad (18)$$

$$V = i\mathcal{H}f \frac{\delta_m}{k} \mu_k, \quad (19)$$

where the logarithmic growth rate is $f = d \ln \delta_m / d \ln a$, $d/d\tau = \mathcal{H}d/d \ln a$, and μ_k is the cosine angle between the line-of-sight direction and the wavevector.

Before we compute the observed galaxy power spectrum, we make a further simplification by ignoring the projected quantities such as the gravitational lensing and the integrated

Sachs-Wolfe contributions in Eqs. (10)–(14), which are important only for the pure transverse modes ($k^\parallel = 0$) [10, 28]. With this simplification and by using Eqs. (9)–(15), the observed galaxy fluctuation in Eq. (3) can be written in Fourier space as

$$\delta_{\text{obs}} = \int \frac{d^3 \mathbf{k}}{(2\pi)^3} e^{i\mathbf{k}\cdot\mathbf{x}} \left[\delta_{\text{Newt}} + \frac{\mathcal{P} \delta_m}{(k/\mathcal{H})^2} - i\mu_k \frac{\mathcal{R} \delta_m}{k/\mathcal{H}} \right], \quad (20)$$

where the two dimensionless coefficients \mathcal{R} and \mathcal{P} are defined as

$$\mathcal{P} = ef - \frac{3}{2} \Omega_m(z) \left[e + f - \frac{1+z}{H} \frac{dH}{dz} + (5p-2) \left(2 - \frac{1}{\mathcal{H}r} \right) \right], \quad (21)$$

$$\mathcal{R} = f \left[e - \frac{1+z}{H} \frac{dH}{dz} + (5p-2) \left(1 - \frac{1}{\mathcal{H}r} \right) \right],$$

and the standard Kaiser formula of the observed galaxy fluctuation is

$$\delta_{\text{Newt}} = b \delta_m - \mu_k^2 \frac{kv}{\mathcal{H}} = (b + f\mu_k^2) \delta_m, \quad (22)$$

which can be contrasted with δ_{obs} in Eq. (3).

Apparent from their spatial dependence in Eq. (20), the coefficients \mathcal{R} and \mathcal{P} originate from the velocity and gravitational potential. While Eq. (3) can be derived with the minimal assumption that the spacetime is described by a perturbed FLRW metric and photons follow geodesics, the coefficient \mathcal{P} in Eq. (21) is obtained by applying the Einstein equations [Eqs. (4)–(6)]. Given the observed e and p , the value and the functional form of \mathcal{P} is, therefore, heavily dependent upon the general theory of relativity.

While \mathcal{P} is purely relativistic, some contributions to \mathcal{R} may be considered non-relativistic, since they could be written down in Newtonian dynamics, simply as a coupling of velocity from the Doppler effect with the time evolution of the galaxy number density. However, different gravity models will yield different values of \mathcal{R} via the logarithmic growth rate f (see, e.g., [29], and further discussion on this issue is presented in Sec. III). Therefore, measuring \mathcal{R} and \mathcal{P} is equivalent to a direct measurement of the relativistic contributions, and we collectively refer to the coefficients \mathcal{R} and \mathcal{P} as the general relativistic effects in the galaxy power spectrum.

Figure 1 illustrates the redshift dependence of two coefficients \mathcal{R} and \mathcal{P} , in which the evolution bias factor is fixed $e = 3$ (constant comoving number density). The contributions to these two coefficients arise from the volume and the source distortions that also involve the change in the observed redshift and the observed flux. Since the volume distortion involves $2\delta r_\chi/r$ in Eq. (3), both coefficients diverge at $z \rightarrow 0$ ($r \rightarrow 0$), unless the radial distortion of the volume effect is cancelled by the source effect ($p = 0.4$), leaving only the distortion terms from the observed redshift (as we show below this cancellation is generic). With $e = 3$ and $p = 0.4$, the coefficient \mathcal{P} in Eq. (21) nearly vanishes at low redshift.

However, as we quantify in Sec. V, even if the divergent term does not cancel out, since the survey volume decreases

faster, the diverging terms have negligible impacts on the measurement significance. Furthermore, Figure 1 appears different from those obtained in [18], since they adopted the halo model to relate the evolution bias factor e to the galaxy bias factor b . Large-scale galaxy surveys show that these two parameters for galaxy samples are independent of each other, and their relation is different from the halo model prediction (e.g., [30]).

Before we close this section, we discuss the fluctuation in the luminosity distance. Additional contribution $5p \delta \mathcal{D}_L$ to the observed galaxy fluctuation arises, because galaxy samples are selected given an observational threshold in flux or equivalently a luminosity threshold L_t converted by using the observed redshift z . For flux-limited samples, the luminosity threshold is changing as a function of redshift, as only brightest galaxies at high redshift can have observed fluxes large enough to be above the threshold in flux. Volume limited samples are constructed by imposing a constant luminosity threshold L_t , up to a maximum redshift. Furthermore, the evolution bias factor e in this case is defined with respect to the number density of galaxies with $L > L_t$, in addition to other criteria such as color cuts.⁵

Fluctuations in luminosity distance bring galaxies around the threshold L_t into (or out of) the galaxy samples, and this effect provides the contribution $5p \delta \mathcal{D}_L$ in Eq. (3). The luminosity function slope of source galaxy populations at the threshold is defined as

$$p = \frac{d \log \bar{n}_g}{dM} = -0.4 \frac{d \log \bar{n}_g}{d \log L} = -0.4 \alpha_L, \quad (23)$$

where the absolute magnitude is related to the luminosity as $M - M_* = -2.5 \log(L/L_*)$ with pivot points M_* and L_* .

The galaxy luminosity function is often described by the Schechter function [31] with a power-law slope α_s and an exponential cut-off as

$$\phi(L)dL = \frac{\phi_*}{L_*} \left(\frac{L}{L_*} \right)^{\alpha_s} \exp \left[-\frac{L}{L_*} \right] dL, \quad (24)$$

and the number density given a threshold in luminosity is then

$$\bar{n}_g(> L_t) = \phi_* \Gamma(\alpha_s + 1, L_t/L_*), \quad (25)$$

where $\Gamma(a, x)$ is the incomplete Gamma function. Therefore, the luminosity function slope at threshold is

$$p = 0.4 \frac{(L_t/L_*)^{\alpha_s+1} \exp \left[-\frac{L_t}{L_*} \right]}{\Gamma(\alpha_s + 1, L_t/L_*)}, \quad (26)$$

which can take values from zero to infinity, depending on the choice of L_t .

A typical case of interest is a flux limited survey, which is dominated by L_* -galaxies at the peak of the luminosity function. For these galaxy samples $p = 0.4$ (solid), which can be obtained with $L_t = L_*$ and $\alpha_s = 0$ (or their variants). These galaxy samples have no diverging terms in \mathcal{R} and \mathcal{P} , because the volume distortion is balanced by the fluctuation in the luminosity distance. We may also assume volume-limited galaxy samples with constant p and consider two additional representative cases in Figure 1. First, galaxy samples at high luminosity tail ($p = 1.5$; dot-dashed), here taken as $L_t = 3L_*$ and for which the Schechter function slope is $\alpha_s \simeq -1.1$ (e.g., [30]). Last, we consider galaxy samples with sufficiently low threshold $L_t \ll L_*$ ($p = 0$; dashed), which contain galaxies at low mass halos.

III. NEWTONIAN CORRESPONDENCE AND REDSHIFT-SPACE DISTORTION

In the cosmological context, full general relativistic equations reduce to Newtonian equations on small scales, in which relativistic effects are negligible. This statement is born out by observations that matter density fluctuations δ in various choices of gauge conditions become identical on small scales, except insofar as unusual gauge conditions are imposed such as the uniform density gauge, in which $\delta \equiv 0$ on all scales. However, as larger scale modes are considered, matter density fluctuations become increasingly different from one another, and the transition scale is largely set by horizon scales $k = \mathcal{H}$.

Even on these large scales, however, ‘‘Newtonian correspondence’’ exists in certain circumstances, in the sense that the matter density δ_m , the velocity v , and the potential ϕ fluctuations in Newtonian dynamics are identical to those quantities in fully relativistic dynamics with certain choices of gauge conditions [25, 27]. In a flat universe with pressureless medium, the Newtonian matter density δ_m is identical to the comoving gauge matter density δ_v , and the Newtonian velocity v and potential ϕ are identical to the conformal Newtonian gauge quantities v_χ and φ_χ . Since this correspondence holds on all scales, numerical simulations properly capture large scale modes [32, 33], apart from other technical issues such as finite box size.

In redshift-space distortion literature [1, 2], a Newtonian calculation has been performed for obtaining the galaxy fluctuation field δ_z in redshift-space that goes beyond the Kaiser formula in Eq. (22). A different notational convention is often adopted in the redshift-space distortion literature. Especially, galaxy number densities n_g are expressed in comoving space.⁶ The selection function α is defined with respect to the

⁵ The luminosity function naturally evolves in time due to aging stars in galaxies, galaxy mergers, cosmic expansion, and so on. However, the condition that $e = 3$ and p is constant relies on the assumption that the shape of the luminosity function at constant L_t remains unchanged, while the physical number density $\bar{n}_g(> L_t)$ is diluted as due to cosmic expansion.

⁶ Conversion of physical quantities to quantities in comoving space requires a redshift parameter. In observation, the observed redshift can be used without gauge ambiguity, but in general a redshift parameter is defined in conjunction with the expansion factor in a homogeneous universe. Therefore, it is a function of coordinate time and hence is gauge-dependent. Only in this section, did we use n_g to refer to the galaxy number density in comoving space, as there is no gauge ambiguity in the Newtonian limit.

comoving number density \bar{n}_g of galaxies as

$$\alpha \equiv \frac{d \ln r^2 \bar{n}_g}{d \ln r} = 2 + \frac{rH}{1+z} (e-3), \quad (27)$$

and the line-of-sight velocity \mathcal{V} is

$$\mathcal{V} \equiv \frac{1+z}{H} V \simeq \frac{1+z}{H} \delta z_\chi, \quad (28)$$

where the last equality holds if we ignore potential contributions to δz_χ in Eq. (10). As a special case, the constant comoving number density $e = 3$ corresponds to $\alpha = 2$, and both of them are constant.

The redshift-space distance s at the observed redshift z is then related to the “real” distance r as

$$s \equiv \int_0^z \frac{dz'}{H} = r + \frac{1+z}{H} \delta z \simeq r + \mathcal{V}, \quad (29)$$

where the first equality is exact to the linear order in perturbation, while the second equality neglects potential contributions to δz .⁷ From the conservation of total number of observed galaxies $n_z(s)d^3s = n_r(r)d^3r$, one derives the relation between the redshift-space and the real-space fluctuations as

$$1 + \delta_z = \frac{\bar{n}_g(r)}{\bar{n}_g(s)} \left| \frac{d^3s}{d^3r} \right| = \frac{r^2 \bar{n}_g(r)}{s^2 \bar{n}_g(s)} \left(1 + \frac{\partial \mathcal{V}}{\partial r} \right)^{-1} (1 + b \delta_m), \quad (30)$$

and to the linear order in perturbations the galaxy fluctuation in redshift-space is then

$$\begin{aligned} \delta_z &= b \delta_m - \left(\frac{\partial}{\partial r} + \frac{\alpha}{r} \right) \mathcal{V} \\ &= b \delta_m - \frac{1+z}{H} \frac{\partial V}{\partial r} - e V + 2V - \frac{2V}{\mathcal{H}r} + \frac{1+z}{H} \frac{dH}{dz} V. \end{aligned} \quad (31)$$

This equation is known as the complete formula for the observed galaxy fluctuation in the redshift-space distortion literature, while only the first two terms constituting the Kaiser formula [1] are often used. The additional terms come from the Jacobian of the transformation from real space to redshift space and also from the galaxy number density evaluated at the observed redshift.

Even with the knowledge of the Newtonian correspondence, there are fewer terms in Eq. (31) compared to the full relativistic formula δ_{obs} in Eq. (3), and those terms account for missing physics in the derivation. Apparently ignored are the fluctuation $\delta \mathcal{D}_L$ in the luminosity distance (effectively $p = 0$) and the lensing contribution that gives rise to distortions between the observed and the source angular positions. Note that this by itself is an important effect: in a generic flux limited survey with $p = 0.4$ the potentially divergent term

$\frac{\alpha}{r} \mathcal{V}$ is exactly cancelled by the luminosity fluctuation effect, which is caused by the fact that a galaxy moved to a redshift closer to the observer will have its flux slightly smaller than what the redshift distance predicts, so it may not enter into a flux threshold, which compensates for the volume effect in the $p = 0.4$ case.

However, once we account for luminosity threshold effects, the Newtonian calculation can fully reproduce the velocity terms in Eq. (3). While the velocity terms receive a relativistic contribution [12] from the gradient of the potential in Eq. (15), it is cancelled by the time derivative of the velocity via the conservation (Euler) equation in Eq. (7). Therefore, the functional form of V is generic in Eq. (3), same in all gravity theories (the conservation equations should hold in other theories of modified gravity, as it simply states that the energy-momentum is locally conserved [34]). However, as we scale the velocity terms with the matter density δ_m by using the Poisson equation (and also the conservation equation), the value of \mathcal{R} itself will be different in other gravity theories than general relativity, and its measurements can test general relativity, although this kind of tests can be performed by using the redshift-space distortion term in δ_{Newt} .

With respect to the relativistic contributions, adding the lensing contribution to the conservation relation in Eq. (31) is still not enough to recover the relativistic formula in Eq. (3). While the lensing contribution accounts for angular distortions, there exist a radial distortion in the source position, the Sachs-Wolfe effect [35] in the observed redshift, and finally the difference in the observer and the galaxy rest frames. Equation (31) can be obtained from the relativistic formula in Eq. (3) by ignoring potential contributions, assuming $p = 0$, and identifying the matter density and the line-of-sight velocity with those in the comoving and the conformal Newtonian gauges, respectively. However, the validity of the Newtonian description on large scales can only be judged retroactively, after the relativistic description is derived. We emphasize again that a fully relativistic treatment is required for estimating \mathcal{P} .

IV. MULTI-TRACER SHOT NOISE CANCELLING TECHNIQUE

We consider multiple galaxy samples with different bias factors for measuring the general relativistic effects in the galaxy power spectrum. Using a vector notation, the observed galaxy fluctuation fields can be written as

$$\begin{aligned} \delta_{\text{GR}}^{\text{obs}} &= \left[\mathbf{b}_0 + f \mu_k^2 \mathbf{I} + \frac{c_{\mathcal{P}} \mathcal{P}}{(k/\mathcal{H})^2} - i \mu_k \frac{c_{\mathcal{R}} \mathcal{R}}{k/\mathcal{H}} \right] \delta_v + \varepsilon \\ &\equiv \mathbf{b}(k, \mu_k) \delta_v + \varepsilon. \end{aligned} \quad (32)$$

where \mathbf{b}_0 , \mathbf{I} , ε are the linear bias, the multi-dimensional identity, and the residual-noise field vectors. By definition the noise-field is independent of the matter fluctuation $\langle \varepsilon \delta_v \rangle = 0$, and the square bracket in Eq. (32) defines the effective bias vector \mathbf{b} . We will adopt a plane parallel approximation for the power spectrum analysis, meaning there is only one angle μ_k

⁷ Since the real distance r takes a gauge-dependent redshift parameter \bar{z} as an argument, we left the gauge choice of δz unspecified, $1+z = (1+\bar{z})(1+\delta z)$.

between the Fourier mode and the line-of-sight direction we need to consider. The corrections to this approximation are expected to be small [8]. More generally, the effects considered here are different from the plane parallel approximation and can be considered separately.

The coefficients \mathcal{P} and \mathcal{R} in Eq. (21) are also generalized to the multi-tracer case as

$$\mathcal{P} = \mathbf{e}f - \frac{3}{2}\Omega_m(z) \left[\mathbf{e} + \left(f - \frac{1+z}{H} \frac{dH}{dz} \right) \mathbf{I} + (5\mathbf{p} - 2\mathbf{I}) \left(2 - \frac{1}{\mathcal{H}r} \right) \right], \quad (33)$$

$$\mathcal{R} = f \left[\mathbf{e} - \frac{1+z}{H} \frac{dH}{dz} \mathbf{I} + (5\mathbf{p} - 2\mathbf{I}) \left(1 - \frac{1}{\mathcal{H}r} \right) \right].$$

We introduced two new parameters $c_{\mathcal{R}}$ and $c_{\mathcal{P}}$ to generalize the measurement significance of the coefficients \mathcal{R} and \mathcal{P} to the case of multiple galaxy samples — they are $c_{\mathcal{R}} = c_{\mathcal{P}} = 1$ in general relativity, and measurements of these two parameters amount to the measurement significance of the two vectors \mathcal{R} and \mathcal{P} .

In order to assess our ability to measure the general relativistic effects in the galaxy power spectrum, we employ the Fisher information matrix, and the likelihood of the measurements is

$$\mathcal{L} = \frac{1}{(2\pi)^{N/2} (\det \mathbf{C})^{1/2}} \exp \left[-\frac{1}{2} \boldsymbol{\delta}_{\text{GR}}^{\text{obs}\dagger} \mathbf{C}^{-1} \boldsymbol{\delta}_{\text{GR}}^{\text{obs}} \right], \quad (34)$$

where the covariance matrix is $\mathbf{C} = \langle \boldsymbol{\delta}_{\text{GR}}^{\text{obs}} \boldsymbol{\delta}_{\text{GR}}^{\text{obs}\dagger} \rangle = \mathbf{b}\mathbf{b}^\dagger P_m + \boldsymbol{\mathcal{E}}$, the shot noise matrix is $\boldsymbol{\mathcal{E}} = \langle \boldsymbol{\varepsilon} \boldsymbol{\varepsilon}^\dagger \rangle$, and the matter power spectrum in the comoving gauge is $P_m(k)$. Since the observed galaxy fluctuation fields are constructed to have a vanishing mean $\langle \boldsymbol{\delta}_{\text{GR}}^{\text{obs}} \rangle = 0$, the Fisher information matrix is

$$F_{ij} = \left\langle -\frac{\partial^2 \ln \mathcal{L}}{\partial \theta_i \partial \theta_j} \right\rangle = \frac{1}{2} \text{Tr} \left[\mathbf{C}^{-1} \mathbf{C}_i \mathbf{C}^{-1} \mathbf{C}_j \right], \quad (35)$$

with two measurement significance parameters $\theta_i = c_{\mathcal{P}}, c_{\mathcal{R}}$ and two nuisance parameter vectors $\theta_i = \mathbf{e}, \mathbf{p}$. The covariance matrix with subscript is $\mathbf{C}_i = \partial \mathbf{C} / \partial \theta_i$.

The inverse covariance matrix of the multi-tracer field and the derivative of the covariance matrix are

$$\mathbf{C}^{-1} = \boldsymbol{\mathcal{E}}^{-1} - \frac{\boldsymbol{\mathcal{E}}^{-1} \mathbf{b}\mathbf{b}^\dagger \boldsymbol{\mathcal{E}}^{-1} P_m}{1 + \alpha}, \quad (36)$$

$$\mathbf{C}_i = \frac{\partial \mathbf{C}}{\partial \theta_i} = \left(\mathbf{b}_i \mathbf{b}^\dagger + \mathbf{b}\mathbf{b}_i^\dagger \right) P_m,$$

where $\alpha = \mathbf{b}^\dagger \boldsymbol{\mathcal{E}}^{-1} \mathbf{b} P_m$, $\mathbf{b}_i = \partial \mathbf{b} / \partial \theta_i$, and we ignored the derivative of the shot noise matrix. With the inverse covariance matrix, we have

$$\begin{aligned} \mathbf{C}^{-1} \mathbf{C}_i \mathbf{C}^{-1} \mathbf{C}_j &= P_m^2 \left(\mathbf{C}^{-1} \mathbf{b}\mathbf{b}_i^\dagger \mathbf{C}^{-1} \mathbf{b}\mathbf{b}_j^\dagger + \mathbf{C}^{-1} \mathbf{b}\mathbf{b}_i^\dagger \mathbf{C}^{-1} \mathbf{b}_j \mathbf{b}^\dagger \right. \\ &\quad \left. + \mathbf{C}^{-1} \mathbf{b}_i \mathbf{b}^\dagger \mathbf{C}^{-1} \mathbf{b}\mathbf{b}_j^\dagger + \mathbf{C}^{-1} \mathbf{b}_i \mathbf{b}^\dagger \mathbf{C}^{-1} \mathbf{b}_j \mathbf{b}^\dagger \right), \end{aligned} \quad (37)$$

and the Fisher information matrix is

$$\begin{aligned} F_{ij} &= (\mathbf{b}^\dagger \mathbf{C}^{-1} \mathbf{b}) \text{Re} \left(\mathbf{b}_i^\dagger \mathbf{C}^{-1} \mathbf{b}_j \right) P_m^2 \\ &\quad + \text{Re} \left[(\mathbf{b}^\dagger \mathbf{C}^{-1} \mathbf{b}_i) (\mathbf{b}^\dagger \mathbf{C}^{-1} \mathbf{b}_j) \right] P_m^2. \end{aligned} \quad (38)$$

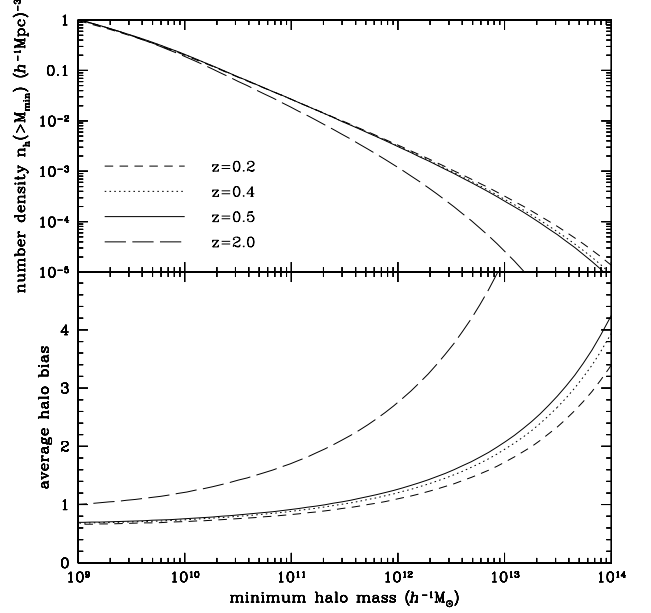


FIG. 2: Number density and average bias of halos above the minimum mass at different redshift slices. Since the multi-tracer method utilizes all the halos of mass above the minimum mass, a large number of halos are required to achieve sufficiently low minimum mass.

To further simplify the equation, we define two more coefficients

$$\beta_i = \mathbf{b}^\dagger \boldsymbol{\mathcal{E}}^{-1} \mathbf{b}_i P_m, \quad (39)$$

$$\gamma_{ij} = \text{Re} \left(\mathbf{b}_i^\dagger \boldsymbol{\mathcal{E}}^{-1} \mathbf{b}_j \right) P_m = \frac{\mathbf{b}_i^\dagger \boldsymbol{\mathcal{E}}^{-1} \mathbf{b}_j + \mathbf{b}_j^\dagger \boldsymbol{\mathcal{E}}^{-1} \mathbf{b}_i}{2} P_m,$$

and the various terms in Eq. (38) are

$$\mathbf{b}^\dagger \mathbf{C}^{-1} \mathbf{b} P_m = \frac{\alpha}{1 + \alpha}, \quad (40)$$

$$\mathbf{b}^\dagger \mathbf{C}^{-1} \mathbf{b}_i P_m = \frac{\beta_i}{1 + \alpha},$$

$$\text{Re} \left(\mathbf{b}_i^\dagger \mathbf{C}^{-1} \mathbf{b}_j \right) P_m = \gamma_{ij} - \frac{\beta_i^* \beta_j + \beta_j^* \beta_i}{2(1 + \alpha)}.$$

The Fisher information matrix is therefore

$$F_{ij} = \frac{\alpha}{1 + \alpha} \gamma_{ij} + \frac{\text{Re}(\beta_i \beta_j - \alpha \beta_i \beta_j^*)}{(1 + \alpha)^2}. \quad (41)$$

This formula is a straightforward extension of the Fisher matrix in [14] with the effective bias vector \mathbf{b} being a complex vector. The imaginary part arises solely from the \mathcal{R} -term in Eq. (32) and its derivative.

For comparison, we also consider measurements by using a single galaxy sample. The formalism presented in Sec. IV is valid for a single tracer, in which vector quantities reduce to scalar quantities. The Fisher information matrix for a single tracer is

$$F_{ij} = \frac{2 \text{Re}(\beta_i) \text{Re}(\beta_j)}{(1 + \alpha)^2}, \quad (42)$$

where we used the relation

$$\alpha\gamma_{ij} = \frac{\beta_i\beta_j^* + \beta_i^*\beta_j}{2}, \quad (43)$$

only valid for a single tracer. Note that in the single tracer we are not sensitive to the correlation between real and imaginary part of the mode, which has the dominant contribution to the signal-to-noise ratio of \mathcal{R} in multi-tracer method [12]. This is only true in the plane parallel approximation.

V. MEASUREMENT SIGNIFICANCE

For definiteness, we consider full sky surveys with three different redshift ranges and adopt a set of cosmological parameters consistent with the WMAP7 results [36]. Given the survey volume V , the Fisher matrix is summed over the Fourier volume, where $k_{\min} = 2\pi/V^{1/3}$ and $k_{\max} = 0.03h\text{Mpc}^{-1}$ (we clarify the dependence of the measurement significance on our choice of k_{\min} and k_{\max}). To model the Fisher matrix parameters α , β_i , γ_{ij} , we adopt the halo model description in [14, 15]; It has been well tested against a suite of N -body simulations with Gaussian and non-Gaussian initial conditions.

We assume that the galaxy samples are constructed to have a constant comoving number density ($e = 3\mathbf{I}$) in a volume-limited survey (constant $\mathbf{p} = p\mathbf{I}$). While uncertainties in e and \mathbf{p} can propagate to the measurement uncertainties in \mathcal{P} and \mathcal{R} , we focus on how well future surveys can measure \mathcal{P} and \mathcal{R} , assuming there are no uncertainties in theoretical predictions of \mathcal{P} and \mathcal{R} . Given the current measurement uncertainties in e and \mathbf{p} [30], the uncertainties in theoretical predictions are very small and will be smaller in future surveys. Figure 2 shows the number density and average bias of halos of mass above the minimum mass M_{\min} at different redshift slices. As we are interested in applying the multi-tracer method with sufficiently low minimum mass to enhance the measurement significance of the general relativistic effects, we consider two cases for the luminosity function slope at the threshold: $p = 0$ (sufficiently low threshold $L_t \ll L_*$) and $p = 0.4$ ($L_t \simeq L_*$).

A. Single tracers

First, we consider the prospect of measuring the general relativistic effects by using a single tracer. Figure 3 shows the predicted measurement significance of \mathcal{R} and \mathcal{P} for various survey redshift ranges. For all galaxy samples with different minimum mass (or different number density in Figure 2), the predicted measurement significance is very weak, indicating that substantial difficulty is present in measuring the general relativistic effects in the galaxy power spectrum for surveys at $z < 3$. This difficulty is simply due to the small number of large-scale modes that are sensitive to the general relativistic effects. Furthermore, the weak measurement significance of both \mathcal{R} and \mathcal{P} means that compared to the standard Newtonian contribution δ_{Newt} , the general relativistic effects or

additional terms in δ_z [Eq. (31)] used in the redshift-space distortion literature are all negligible in the standard power spectrum analysis (single tracer method).

This result confirms the prediction in [10] and extends the predictions to galaxy samples with different number density and bias. This conclusion is in apparent contradiction with [6], where correlation functions are shown with smaller errors than the size of the effects. However, these errors are obtained from simulations without taking into account the actual number of modes in a realistic survey. Once this is taken into account there is no contradiction [8]. The reason the wide-angle correction remains small is that there exists no velocity-density correlation ($\sim \mathcal{R}$) due to symmetry of pairs in Eq. (20) and the effect shows up only as a correction to the dominant contributions that are already accounted in the plane-parallel limit.

The difference in the predicted measurement significance between the left ($p = 0.0$) and the right ($p = 0.4$) panels arise from the redshift dependence of the \mathcal{R} and \mathcal{P} values, as illustrated in Figure 1. The signals are computed at the mean redshift of each survey, and in the left panel ($p = 0.0$), the absolute values of \mathcal{R} and \mathcal{P} slowly decrease with redshift, while they remain nearly constant in the right panel ($p = 0.4$). Furthermore, even with higher suppression power of (k/\mathcal{H}) , it is generally easier to measure \mathcal{P} than \mathcal{R} in the single tracer method for the case with $p = 0.0$ (left panel). Arising from the imaginary part in Eq. (32), the \mathcal{R} -term in the galaxy power spectrum is negligible, compared to the real part that includes the standard Newtonian term and the \mathcal{P} -term, while the sensitivity to the \mathcal{P} -term comes from the cross-correlation of the standard Newtonian term and the \mathcal{P} -term. In the left panel, the lack of sensitivity to the \mathcal{P} -term is due to the vanishing signal of \mathcal{P} .

While the shot noise of massive halos is an obstacle for measuring the general relativistic effects, it is the cosmic variance on large scales that fundamentally limits the measurement significance. Therefore, the measurement significance slowly increases as the minimum halo mass is lowered, but it quickly saturates given values of \mathcal{R} and \mathcal{P} . For measuring the general relativistic effects in the galaxy power spectrum, there is no further gain in constructing galaxy samples with large number density at a fixed survey volume.

B. Multiple tracers

This conclusion is, however, contingent upon the assumption that the power spectrum analysis is performed by using a single tracer, and the multi-tracer method can change the prospect of measuring the general relativistic effects in a dramatic way. Figure 4 shows the predicted measurement significance of the general relativistic effects by taking full advantage of the multi-tracer method. Compared to the single tracer case in Figure 3, there exist two key differences in the measurement significance derived by using the multi-tracer method. First, the measurement significance is greatly enhanced in Figure 4 by eliminating the cosmic variance, which sets the fundamental limit in the single tracer method. Sec-

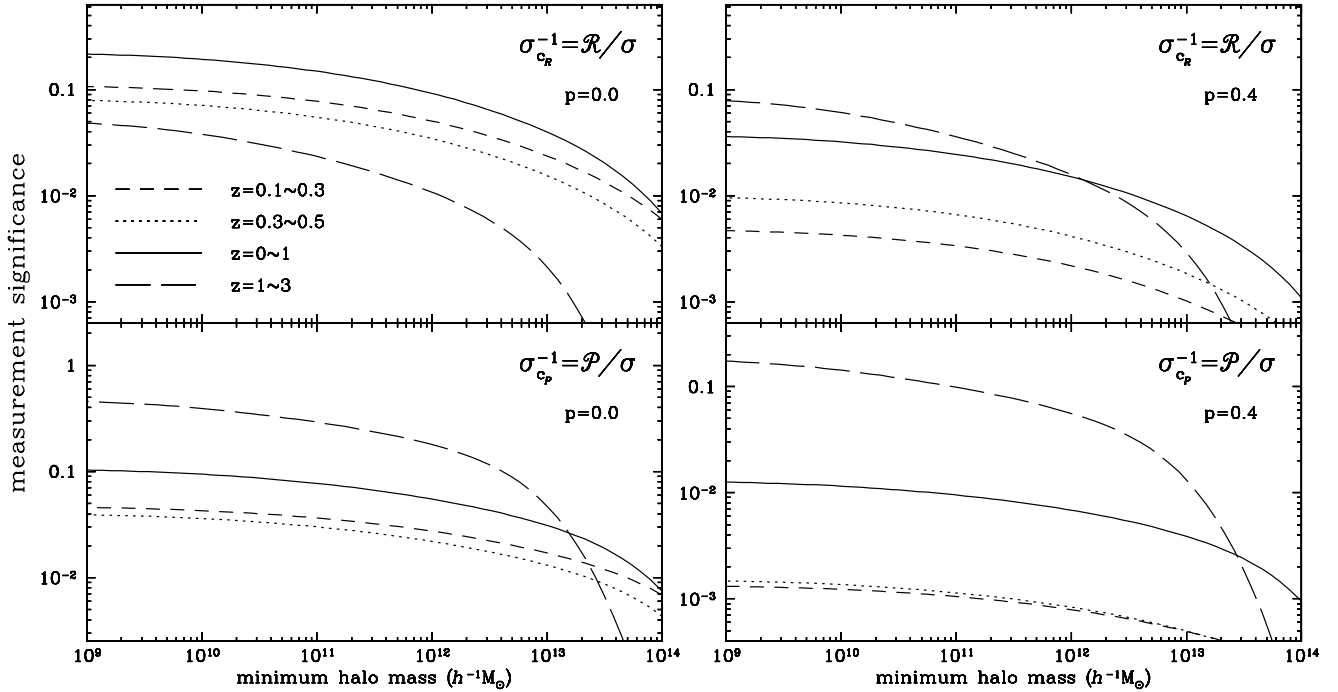


FIG. 3: Predicted measurement significance of general relativistic effects \mathcal{R} (upper) and \mathcal{P} (bottom) in the galaxy power spectrum obtained by using a single tracer. All halos of mass above minimum mass are lumped together to construct a single tracer. Four curves represent different survey redshift ranges with corresponding volume $V = 2.5, 7.9, 59, 410 (h^{-1}\text{Gpc}^3)^3$. For the volume-limited sample (constant p) with constant comoving number density ($e = 3$), two galaxy samples are constructed to have $p = 0$ (left) and $p = 0.4$ (right). No uncertainties in theoretical predictions are assumed. With the traditional power spectrum analysis (single tracer), it is difficult to measure the general relativistic effects at any meaningful significance.

ond, a substantially larger measurement significance of the \mathcal{R} -term is obtained than that of the \mathcal{P} -term by cross-correlating multiple galaxy samples and thereby isolating the imaginary term [12]. The method of measuring the imaginary part in the galaxy power spectrum of two tracers [12] is fully implemented in our complex covariance matrix as off-diagonal terms and extended to the number of tracers larger than two. The result in [12] would correspond to $\mathcal{R}/\sigma \simeq 1.8$ at $z \leq 1$.

In our most optimistic scenario, if we can utilize all halos of $M \geq 10^{12}h^{-1}M_{\odot}$, the velocity term \mathcal{R} (solid) of the galaxy samples with $p = 0$ (left panel) can be measured at more than $10\text{-}\sigma$ confidence level at $z \leq 1$, while it is still difficult to detect the gravitational potential term \mathcal{P} (solid). A significant detection of \mathcal{R} can be made, even in surveys at low redshift (dotted and short-dashed), if halos of $M < 10^{12}h^{-1}M_{\odot}$ can be used. At higher redshift $z \geq 1$, though the increase in the survey volume is partially cancelled by the lower abundance of halos at a fixed mass, a substantial improvement (dashed) for \mathcal{P} can be achieved by going beyond $z = 1$, as the signal \mathcal{P} increases with redshift ($p = 0$).

However, the scenario above is not very realistic because of the $p = 0$ assumption. In the right panels, we consider the galaxy samples with $p = 0.4$, of which the \mathcal{R} and \mathcal{P} values are nearly constant at all redshifts. The constant signals result in

higher measurement significance for surveys with larger volume at higher redshift. Compared to the case with $p = 0.0$, the measurement significance of \mathcal{R} is smaller due to the smaller value of \mathcal{R} at $z < 1$, while that of \mathcal{P} is highly suppressed due to the vanishing value of \mathcal{P} . By using halos of mass slightly lower than $10^{12}h^{-1}M_{\odot}$, a survey like the BOSS that covers redshift range $z = 0.3 \sim 0.5$ with a quarter of the sky can achieve a $1\text{-}\sigma$ detection of \mathcal{R} , demonstrating the feasibility of the multi-tracer analysis in future surveys.

A few caveats are in order. First, we used the galaxy power spectrum in a flat-sky and counted the number of modes in computing the measurement significance. Calculations of wide-angle correlation functions [8] shows that the effects of geometry are negligible, and a similar calculation can be performed for power spectrum measurements (in preparation). Furthermore, our calculation is rather insensitive to the minimum wavenumber k_{\min} . At sufficiently low M_{\min} , the multi-tracer method approaches the optimal case with dark matter density field, where the Fisher information can be approximated as $\mathbf{b}'\mathcal{E}^{-1}\mathbf{b}'P_m$. In terms of spatial dependence alone in Eq. (32), $F_{\mathcal{P}} \propto \int dk k^2 (k^n/k^4) \propto \ln(k_{\max}/k_{\min})$ and $F_{\mathcal{R}} \propto \int dk k^2 (k^n/k^2) \propto (k_{\max}^2 - k_{\min}^2)$ with the spectral index $n \simeq 1$. Therefore, the dependence of the measurement significance on k_{\min} is logarithmic for \mathcal{P} and negligible for \mathcal{R} ,

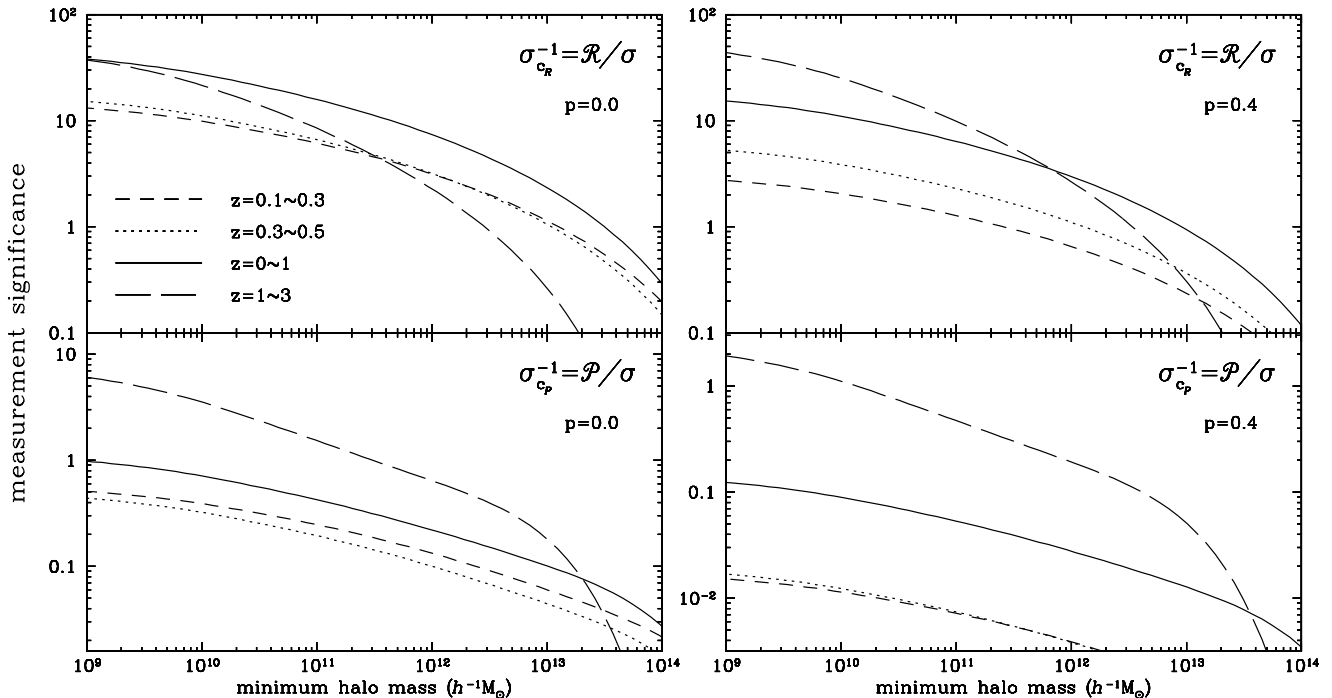


FIG. 4: Predicted measurement significance of general relativistic effects \mathcal{R} (upper) and \mathcal{P} (bottom) in the galaxy power spectrum derived by using the multi-tracer method. All halos of mass above minimum mass are utilized to take advantage of the multi-tracer method [11, 14]. Various curves are in the same format as in Figure 3. Compared to Figure 3, the measurement significance is substantially enhanced by using the multi-tracer method.

as $k_{\max} \gg k_{\min}$. In contrast, a significance enhancement in $F_{\mathcal{R}}$ can be achieved by increasing the maximum wavenumber k_{\max} , although the gain is marginal for $F_{\mathcal{P}}$. Finally, while any degeneracy with cosmological parameters in measuring the relativistic effects is largely eliminated due to the cancellation of the underlying matter distribution [11, 14], a proper quantification of the measurement significance requires considerations of uncertainties in theoretical predictions of \mathcal{P} and \mathcal{R} .

VI. PRIMORDIAL NON-GAUSSIANITY

We extend our formalism to the primordial non-Gaussian signature in galaxy bias [37] and introduce additional parameter f_{NL} . Here we only consider the simplest local form of primordial non-Gaussianity to demonstrate how it can be implemented in the general relativistic description, and ignore scale-independent and scale-dependent corrections (see, e.g., [38–40]).

The primordial non-Gaussian signature in galaxy bias can be readily implemented in our full general relativistic description with the Gaussian bias factor in Eq. (3) replaced by

$$b \rightarrow b + 3f_{\text{NL}}(b-1)\delta_c \frac{\Omega_m(z)\mathcal{H}^2}{T_\varphi(k,z)k^2}, \quad (44)$$

where δ_c is the linear overdensity for spherical collapse and T_φ is the transfer function of the curvature perturbation (see also [18, 19, 22]). Equivalently, the primordial non-Gaussianity can be considered as additional relativistic contribution by replacing \mathcal{P} in Eq. (21) with

$$\mathcal{P}_{f_{\text{NL}}} = \mathcal{P} + 3f_{\text{NL}}(b-1)\delta_c \frac{\Omega_m(z)}{T_\varphi(k,z)}. \quad (45)$$

Figure 5 shows the predicted constraints on the primordial non-Gaussianity derived by accounting for the full general relativistic effects. In obtaining the constraint $\sigma_{f_{\text{NL}}}$ on primordial non-Gaussianity, we set $c_{\mathcal{R}} = c_{\mathcal{P}} = 1$ and marginalize over e and p with priors $\sigma_e = 0.1$ and $\sigma_p = 0.05$ [30]. We emphasize that e and p can be more accurately measured in observations, further reducing their uncertainties. With the current uncertainties in e and p , the constraint $\sigma_{f_{\text{NL}}}$ (solid in Fig. 5) is nearly identical to the unmarginalized constraint. The dashed curve shows that even with no priors on e and p , $\sigma_{f_{\text{NL}}}$ is not inflated except in the regime with $\sigma_{f_{\text{NL}}} \lesssim 2$, because \mathcal{R} and \mathcal{P} are affected simultaneously by e and p but only \mathcal{P} by f_{NL} . Furthermore, the unique dependence of f_{NL} on $b-1$ and T_φ in Eq. (44) provides the multi-tracer method with more leverage to separate it from the general relativistic effect. It is the primordial gravitational potential at initial epoch, not the evolved gravitational potential at the observed redshift that the scale-dependent galaxy bias responds to, and the difference is

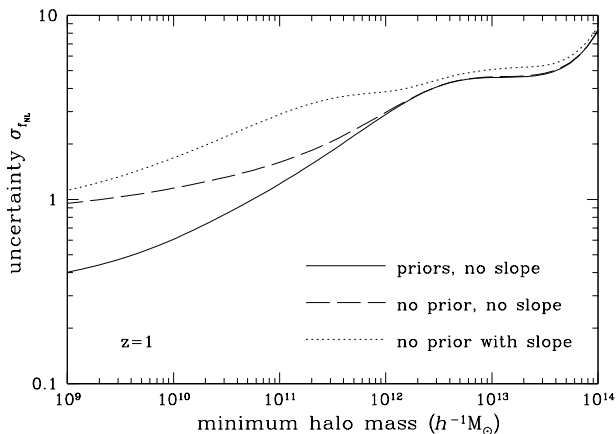


FIG. 5: Predicted constraints on the primordial non-Gaussianity f_{NL} from galaxy power spectrum measurements. To facilitate the comparison, the constraints on f_{NL} are obtained by using the same survey specifications as in [14]: $V \simeq 50 (h^{-1}\text{Gpc})^3$ centered at $z = 1$. We assume $e = 3$ and $p = 0.4$, and various curves show $\sigma_{f_{\text{NL}}}$ with different priors on e and p ($\sigma_e = 0.1$, $\sigma_p = 0.05$ [30] for the solid curve).

the transfer function $T_\varphi(k, z)$. At low redshift, the transfer function decays from unity on scales smaller than the horizon around the dark energy domination epoch, and there exists a factor two difference in $T_\varphi(k, z)$ at our adopted k_{max} .

Finally, we allow e and p to vary as a function of mass with two logarithmic slope parameters α_e and α_p :

$$\begin{aligned} e &= e_0 \mathbf{I} + \alpha_e \ln(M/M_0), \\ p &= p_0 \mathbf{I} + \alpha_p \ln(M/M_0), \end{aligned} \quad (46)$$

with $e_0 = 3$, $p_0 = 0.4$, $\alpha_e = \alpha_p = 0$, and $M_0 = 10^{12} h^{-1} M_\odot$. The effects of α_e and α_p (dotted in Fig. 5) are sufficiently different from that of f_{NL} , and $\sigma_{f_{\text{NL}}}$ asymptotically reaches the floor set by the uncertainties in e and p . This demonstrates that the general relativistic effects in the galaxy power spectrum are *not* degenerate with the primordial non-Gaussian signature. However, if f_{NL} were to be constrained below unity, similar precision needs to be achieved in predicting \mathcal{R} and \mathcal{P} .

This requirement can be relaxed by increasing the maximum wavenumber k_{max} to exploit the unique dependence of f_{NL} on $T_\varphi(k, z)$. With larger maximum wavenumber $k_{\text{max}} = 0.1 h \text{Mpc}^{-1}$, the overall uncertainties on f_{NL} are reduced by about 30% for all three cases in Figure 5. Another way is to construct galaxy samples by using independent mass estimates instead of observed flux, as p drops out in Eq. (20), further separating e from f_{NL} .

VII. DISCUSSION

In this paper we explore the contributions to the redshift survey beyond the Kaiser approximation in the context of recently developed general relativistic analysis. We compare the results of this formalism to the previous analyses [6] and

show that these analyses ignore several terms such as luminosity distance fluctuation and overestimate the significance of the effect. In addition, correlation function analyses previously adopted are not optimal to assess the signal-to-noise ratio of these effects, in contrast to our power spectrum analysis. We find that these corrections beyond the Kaiser formula are not observable in a generic redshift survey using a single tracer, meaning that these effects do not have to be considered in a generic redshift survey. A caveat to this conclusion is that in this paper we have performed the analysis using the plane parallel approximation and do not consider large angle effects [3, 4], but we expect that these effects are equally small [8]. Their detectability will be addressed in a separate publication.

Using the multi-tracer shot noise cancelling method the detection significance is increased, providing a unique opportunity to test these effects, and general relativity in general, on horizon scales. Still, for realistic cases the detection significance is at the few sigma confidence level (in some more optimistic cases the detectability rises to 10 sigma or more), so this test of general relativity is of interest only when the deviations from general relativity are significant on large scales. We have also shown how the primordial non-Gaussian effect in galaxy bias can be implemented in the full general relativistic description, and we have argued that the ability to detect primordial non-Gaussianity is little compromised by the presence of general relativistic effects.

Considering the fact that we perform a very large-scale analysis, our method of measuring the general relativistic effects in galaxy clustering need not be restricted to spectroscopic surveys. The use of photometric redshift measurements may not affect our results if the photo- z error is sufficiently small, e.g. an error of $dz/(1+z) \sim 0.03$ corresponds to $k > 0.06 h \text{Mpc}^{-1}$ at $z = 1$, which is larger than $k_{\text{max}} = 0.03 h \text{Mpc}^{-1}$ we adopted here. This allows one in principle to extend the observed halo mass ranges to lower masses using a photometric survey and to take full advantage of the multi-tracer method.

While we treated multiple galaxy samples as halos in multiple mass bins and our method requires sufficiently low M_{min} , the SDSS already measures galaxies well below $M = 10^{11} h^{-1} M_\odot$ (e.g., SDSS L1 sample), and there exists numerous methods to remove satellite galaxies and isolate central galaxies. Furthermore, it is shown [14] that one needs a fairly large scatter in the mass-observable relation, $\sigma_{\ln M} = 0.5$, to degrade the shot-noise suppression, and the scatter is less important at the low mass end. The reason for this insensitivity to the scatter is that in terms of weighting, the optimal weighting method puts more weight on massive halos, $w(M) = M + M_0$, where M_0 is a constant and approximated as 3 times the minimum mass. We note however that our prediction is based on the halo model description of the shot noise matrix, which is tested only for halos at $M \geq 10^{12} h^{-1} M_\odot$, and our prediction at $M \leq 10^{12} h^{-1} M_\odot$ is an extrapolation.

The bottom line of this paper is that the corrections beyond the Kaiser formula in redshift surveys are generally small and only detectable using very specialized techniques adopted in this paper. This is a good news for those analyzing generic redshift surveys since they do not have to consider them. Nev-

ertheless, the potential detectability of these terms gives rise to the prospect of testing general relativity in a regime previously untested. Thus despite the small detection significance it is worth exploring these tests further to see if they can be of use in separating general relativity from some of its alternatives.

Acknowledgments

We acknowledge useful discussions with Daniel Eisenstein, Lucas Lombriser, and Pat McDonald. J.Y. is supported by

the SNF Ambizione Grant. This work is supported by the Swiss National Foundation under contract 200021-116696/1 and WCU grant R32-10130. M. Z. is supported by the National Science Foundation under PHY-0855425 and AST-0907969 and by the David and Lucile Packard foundation and the John D. and Catherine T. MacArthur Foundation.

-
- [1] N. Kaiser, *Mon. Not. R. Astron. Soc.* **227**, 1 (1987).
- [2] A. J. S. Hamilton, in *The Evolving Universe*, edited by D. Hamilton (1998), vol. 231 of *Astrophysics and Space Science Library*, pp. 185–+.
- [3] A. S. Szalay, T. Matsubara, and S. D. Landy, *Astrophys. J. Lett.* **498**, L1 (1998), arXiv:9712007.
- [4] I. Szapudi, *Astrophys. J.* **614**, 51 (2004), arXiv:0404477.
- [5] P. Pápai and I. Szapudi, *Mon. Not. R. Astron. Soc.* **389**, 292 (2008), arXiv:0802.2940.
- [6] A. Raccanelli, L. Samushia, and W. J. Percival, *Mon. Not. R. Astron. Soc.* **409**, 1525 (2010), arXiv:1006.1652.
- [7] D. Bertacca, R. Maartens, A. Raccanelli, and C. Clarkson (2012), 1205.5221.
- [8] L. Samushia, W. J. Percival, and A. Raccanelli, *Mon. Not. R. Astron. Soc.* **420**, 2102 (2012), arXiv:1102.1014.
- [9] J. Yoo, A. L. Fitzpatrick, and M. Zaldarriaga, *Phys. Rev. D* **80**, 083514 (2009), arXiv:0907.0707.
- [10] J. Yoo, *Phys. Rev. D* **82**, 083508 (2010), arXiv:1009.3021.
- [11] U. Seljak, *Phys. Rev. Lett.* **102**, 021302 (2009), 0807.1770.
- [12] P. McDonald, *J. Cosmol. Astropart. Phys.* **11**, 26 (2009), 0907.5220.
- [13] U. Seljak, N. Hamaus, and V. Desjacques, *Phys. Rev. Lett.* **103**, 091303 (2009), 0904.2963.
- [14] N. Hamaus, U. Seljak, and V. Desjacques, *Phys. Rev. D* **84**, 083509 (2011), 1104.2321.
- [15] N. Hamaus, U. Seljak, V. Desjacques, R. E. Smith, and T. Baldauf, *Phys. Rev. D* **82**, 043515 (2010), 1004.5377.
- [16] C. Bonvin and R. Durrer, *Phys. Rev. D* **84**, 063505 (2011), arXiv:1105.5280.
- [17] A. Challinor and A. Lewis, *Phys. Rev. D* **84**, 043516 (2011), arXiv:1105.5292.
- [18] D. Jeong, F. Schmidt, and C. M. Hirata, *Phys. Rev. D* **85**, 023504 (2012), arXiv:1107.5427.
- [19] T. Baldauf, U. Seljak, L. Senatore, and M. Zaldarriaga, *J. Cosmol. Astropart. Phys.* **10**, 31 (2011), arXiv:1106.5507.
- [20] J. M. Bardeen, *Phys. Rev. D* **22**, 1882 (1980).
- [21] J. Yoo, *Phys. Rev. D* **79**, 023517 (2009), arXiv:0808.3138.
- [22] M. Bruni, R. Crittenden, K. Koyama, R. Maartens, C. Pitrou, and D. Wands, *Phys. Rev. D* **85**, 041301 (2012), arXiv:1106.3999.
- [23] H. Kodama and M. Sasaki, *Progress of Theoretical Physics Supplement* **78**, 1 (1984).
- [24] J.-C. Hwang and H. Noh, *Phys. Rev. D* **65**, 023512 (2001), arXiv:0102005.
- [25] J. Hwang and H. Noh, *Gen. Relativ. Gravit.* **31**, 1131 (1999), arXiv:9907063.
- [26] D. Wands and A. Slosar, *Phys. Rev. D* **79**, 123507 (2009), 0902.1084.
- [27] J.-C. Hwang and H. Noh, *Phys. Rev. D* **72**, 044011 (2005), arXiv:0412128.
- [28] L. Hui, E. Gaztañaga, and M. Loverde, *Phys. Rev. D* **77**, 063526 (2008), arXiv:0710.4191.
- [29] R. Reyes, R. Mandelbaum, U. Seljak, T. Baldauf, J. E. Gunn, L. Lombriser, and R. E. Smith, *Nature* **464**, 256 (2010), 1003.2185.
- [30] R. J. Cool, D. J. Eisenstein, X. Fan, M. Fukugita, L. Jiang, C. Maraston, A. Meiksin, D. P. Schneider, and D. A. Wake, *Astrophys. J.* **682**, 919 (2008), 0804.4516.
- [31] P. Schechter, *Astrophys. J.* **203**, 297 (1976).
- [32] J. Hwang and H. Noh, *Mon. Not. R. Astron. Soc.* **367**, 1515 (2006), arXiv:0507159.
- [33] N. E. Chisari and M. Zaldarriaga, *Phys. Rev. D* **83**, 123505 (2011), 1101.3555.
- [34] E. Bertschinger, *Astrophys. J.* **648**, 797 (2006), arXiv:0604485.
- [35] R. K. Sachs and A. M. Wolfe, *Astrophys. J.* **147**, 73 (1967).
- [36] E. Komatsu, K. M. Smith, J. Dunkley, C. L. Bennett, B. Gold, G. Hinshaw, N. Jarosik, D. Larson, M. R. Nolte, L. Page, et al., *Astrophys. J. Suppl. Ser.* **192**, 18 (2011), 1001.4538.
- [37] N. Dalal, O. Doré, D. Huterer, and A. Shirokov, *Phys. Rev. D* **77**, 123514 (2008), 0710.4560.
- [38] A. Slosar, C. Hirata, U. Seljak, S. Ho, and N. Padmanabhan, *J. Cosmol. Astropart. Phys.* **8**, 31 (2008), 0805.3580.
- [39] V. Desjacques and U. Seljak, *CQG* **27**, 124011 (2010), 1003.5020.
- [40] V. Desjacques, D. Jeong, and F. Schmidt, *Phys. Rev. D* **84**, 061301 (2011), arXiv:1105.3628.